Available online at www.sciencedirect.com
SCIENCE DIRECT®
Journal of Magnetic Resonance 170 (2004) 278–283
JMR Journal of Magnetic Resonance
www.elsevier.com/locate/jmr

Suppression of electron spin-echo envelope modulation peaks in double quantum coherence electron spin resonance

Marco Bonora, James Becker, Sunil Saxena*

Department of Chemistry, University of Pittsburgh, Pittsburgh, PA 15260, USA

Received 14 May 2004; revised 1 July 2004
Available online 31 July 2004

Abstract

We show the use of the observer blind spots effect for the elimination of electron spin-echo envelope modulation (ESEEM) peaks in double quantum coherence (DQC) electron spin resonance (ESR). The suppression of ESEEM facilitates the routine and unambiguous extraction of distances from DQC-ESR spectra. This is also the first demonstration of this challenging methodology on commercial instrumentation.

Keywords: Double quantum ESR; Dipolar interactions; FT-ESR; Distance measurements; Spin-labeling

1. Introduction

Over the last decade Fourier transform (FT) electron spin resonance (ESR) has emerged as an attractive new tool for the measurement of weak magnetic dipolar interactions (100 kHz–15 MHz) between two paramagnetic centers on a macromolecule [1–11]. This has opened up a method for the measurement of interspin separations in the 15–80 Å range, even in amorphous materials. When combined with site-directed spin-labeling [12–15] these FT-ESR experiments provide an exciting methodology for the establishment of global folding patterns and conformational dynamics in proteins [16–18] and nucleic acids [19,20] in order to elucidate structure–function relationships.

Most applications have utilized the methods of double quantum coherence (DQC) [17], double electron–electron resonance (DEER) [16,18,21–25], and the associated pulsed electron double resonance (PELDOR) [2,19,20,26–28]. The spectroscopic effects of weak spin–spin interactions are amplified in these experiments by the use of two different strategies. In DQC FTESR, spin–spin interactions generate a double quantum coherence. The rate of formation of this DQ coherence directly reports on the strength of the dipolar interaction, providing sensitivity to distances. The DEER/PELDOR class of experiments relies on the selective inversion of the local dipolar field due to the coupled-spin partner. The primary echo is then modulated by the dipolar frequency providing sensitivity to distances. Both the DQC and the DEER/PELDOR experiments yield characteristic lineshapes and splittings which may be analyzed for distances and distance distributions.

The two philosophies place different technical requirements on the spectrometer. For effective excitation of the double quantum coherence, high power pulses of a short duration (π of $\leqslant 8$ ns) are optimally required. Such pulses have traditionally been feasible only in homebuilt apparatus and, as such, DQC FTESR has not been demonstrated on commercial instrumentation. With sufficient pulse-power and for concentrated samples (e.g. γ-irradiated fused silica), the intensity of the

* Corresponding author. Fax: 1-412-624-8611.
E-mail address: sksaxena@pitt.edu (S. Saxena).

1090-7807/$ - see front matter © 2004 Elsevier Inc. All rights reserved.
doi:10.1016/j.jmr.2004.07.006

DQC-filtered echo can be as large as 50% of the primary two-pulse echo [29, p. 417].

DEER and PELDOR rely on selective excitation of the ESR spectrum and therefore place lower requirements on pulse lengths and powers (π of ~24–40 ns). However, DEER/PELDOR experiments typically require a second microwave source, although a method that uses a single microwave frequency and simultaneous longitudinal radio frequency excitation has recently been developed [30]. The use of irradiation at two different frequencies minimizes interference from electron spin-echo envelope modulation (ESEEM) due to the electron–nuclear dipolar (END) interaction. In addition, DEER/PELDOR have been generalized to the case of paramagnetic metal centers [21], which has facilitated the determination of structural constraints in metallo-proteins [24,31].

There is no natural way of removing ESEEM in DQC FTESR. In the commonly used nitroxide, the dominant contribution to ESEEM is from END interaction between the electron spins and matrix protons in an aqueous solution. This yields peaks at ~14.7 MHz at a spectrometer resonance frequency of 9.6 GHz (X-band). The 14.7 MHz contribution interferes with the DQC peak from electron spin–spin dipolar interaction when the interspin distance is in the range of 15 Å. One elegant approach around this problem is to perform DQC FTESR at a higher resonance frequency (i.e., ~17 GHz) using novel, custom-built instrumentation [32]. In this case, the ESEEM peak is shifted to about ~26 MHz, which is well outside the range of the dipolar frequencies of interest. Alternatively, ESEEM frequencies may also be cancelled by an appropriate choice of pulse separations and summing of signals collected using different pulse separations [6,17].

In this work, we show that DQC FTESR signals may be routinely obtained using commercial spectrometers. A method based on observer blind spots [33,34] to reduce ESEEM effects in DQC FTESR is presented.

2. Materials and methods

2.1. Samples

A peptide CPPPPPPC (P, proline; C, cysteine) was synthesized at the peptide facility of the University of Pittsburgh. The peptide was spin-labeled on the cysteines with the methanethiosulfonate (MTSSL) spin-label using established procedure [35]. A 0.27 mM solution of the peptide was prepared in 40% glycerol, 30% 2,2,2-trifluoroethanol, and 30% water, buffered to pH 7 using *N*-ethylmorpholine. The second biradical, 2,6-bis-[5-(1-*N*-oxylo-2,2,6,6-tetramethyl-1,3,3,6-tetrahydropyridin-4-yl)-thiophen-2-ylmethylene]-cyclohexanone, labeled R1, was a gift from Prof. Anatoly E. Myshkin and its molecular weight has been confirmed by mass spectroscopy. A 2.5 mM solution of R1 in toluene was used for the DQC-ESR experiments. Each sample (~8 μl) was placed in a 1.5 mm pyrex tube and flash-frozen in liquid nitrogen immediately before insertion into the cavity. All of the experiments were recorded at $T = 80$ K.

2.2. FT-ESR spectroscopy

The ESR experiments were performed on a Bruker EleXsys E580 X-band CW/FT ESR spectrometer operating at resonance frequency of ~9.6 GHz. A Bruker ER4118X-MS3 split ring resonator with a resonator $Q \leqslant 100$ and an ASE TWTA with an output power of 1 kW provided $\pi/2$ and π pulses as short as 6 and 12 ns, respectively. The pulse lengths were determined using an echo nutation experiment. These pulse lengths combined with the resonator bandwidth at 80 K provided a spectral coverage of ~80 MHz. This attenuated coverage reduces the efficiency of creation of DQ coherence, but we show that the experiment is nevertheless feasible.

A six-pulse sequence shown in Fig. 1 was used for the DQC experiments. A basic phase cycle of 64 steps augmented with CYCLOPS for a total of 256 steps [29, pp. 454–455] was used to eliminate all unwanted signals. The volume of the sample that is detected by the split ring resonator is ~7 μl and, in such a small volume, we expect that B_1 is nearly uniform. The phase cycle selectively isolates the DQC signal, removing any effects due to pulse imperfections.

In our implementation of DQC–ESR, a constant time version is not used. Our version introduces homogeneous relaxation (characterized by T_m) and can lead to a loss of resolution for very large distances or for T_m limited samples. This was not an issue for the samples used in this work.

The time-domain signal was digitized using the Bruker SpecJect transient signal averager starting at 16 ns before the top of the echo. A total of 256 points with a resolution of 4 ns were collected to obtain the echo signal as well as a sufficient amount of baseline (cf. Fig. 1B). The data were collected for several values of t_p to yield a two-dimensional data set. For the peptide sample, a total of 256 steps were collected in t_p with a step-size of 16 ns. For the R1 sample, a total of 128 steps were collected in t_p with a step-size of 6 ns. Both experiments had an initial delay in t_p (i.e., dead-time) of 16 ns and the t_1 delay was fixed at 16 ns. The DQC signal was summed for four values of the period, t_2, of 84, 100, 116, and 132 ns. The 16 ns step-size in t_2 corresponds to $1/4\nu_H$, where ν_H is the proton nuclear Larmor frequency. This was done in an attempt to average the proton ESEEM [6,17].

For the peptide sample, the number of averages was 300 and a repetition rate of 1.4 kHz was used. For the R1 biradical, the number of averages was 500 and the

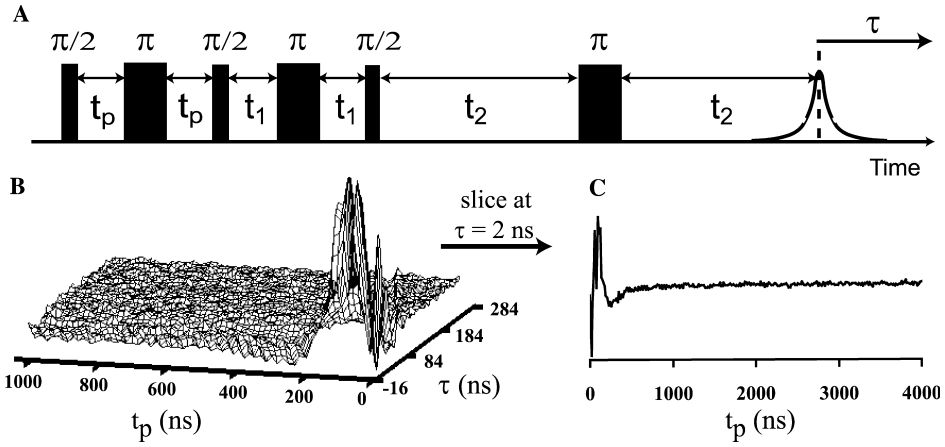

Fig. 1. (A) Pulse sequence for DQC FTESR. In the experiment, t_p (the orthogonal dimension) was stepped out by 6 ns for biradical R1 and by 16 ns for the peptide biradical. The echo signal was digitized starting 16 ns before the top of the echo, with a resolution of 4 ns in the direct dimension, τ, to yield a two-dimensional data set. (B) The 2D time domain data obtained from the peptide sample is shown (for clarity parts of the baseline have been eliminated). We define $\tau = 0$ to lie at the top of the echo. (C) A slice of the DQ signal for $\tau = 2$ ns is shown.

repetition rate was 2 kHz. With these experimental conditions the total acquisition time is typically 16 h (4 h for each t_2 step). It should be noted that, with the step sizes and repetition rates used and for ~300 averages, the experimental time for one value of t_2 should be ~1 h. The acquisition time is currently limited only by slow data transfer rates of the instrumental hardware.

2.3. Data analysis

We use the direct dimension to denote the dimension of data collection (i.e., τ in Fig. 1) and the orthogonal dimension to denote the dimension in which t_p was incremented (see Fig. 1). The experimental two-dimensional time domain data set consists of the echo shape (along τ) versus t_p. Each slice along t_p was phased and the real-part retained. An exponential function was subtracted to remove contributions due to relaxation (see below) and any possible decay due to intermolecular electron–electron interactions [36–38]. An exponential window along t_p with $t_{exp} = 1$ μs was applied on the peptide spectrum. The time domain signal was 1D Fourier Transformed along t_p to yield the DQC spectrum along the ν_p axis.

The method of data collection and analysis employed in this work yields, in essence, a series of single-point detections, i.e., a 1D spectrum for each τ value of the echo. For a given 1D spectrum, this method results in a loss of sensitivity in comparison to integrating the full echo. However, the signal to noise ratio of the digitized DQC signal can be recouped by summing together every 1D slice extracted from the two-dimensional plot, if required.

3. Results and discussion

The time-domain DQC signal along t_p is a combination of three different effects: modulation due to the electron–electron intramolecular dipolar interaction, modulation due to ESEEM [39] from matrix protons, and a homogeneous decay of the echo signal characterized by the phase memory time, T_m, and by intermolecular electron–electron interactions. The contributions to the decay are usually subtracted out digitally (see Section 2) [17,22].

A DQC FTESR spectrum of the poly-proline biradical is shown in Fig. 2. The orthogonal axis displays the DQC spectrum for several slices along the direct dimension. Peaks due to electron–electron dipolar interaction occur at ±2.9 MHz, which corresponds to an average distance of 26.5 Å. This is consistent with the minimized energy configuration calculation using the MMFF94 force field under Molecular Operating Environment (MOE), which yielded a distance between the nitroxide moieties of 28 ± 2 Å [40].

Electron–nuclear dipolar interaction between unpaired electron and matrix protons [41] leads to ESEEM peaks at ±14.7 MHz along ν_p. These are displayed more clearly in Fig. 2B, which shows the DQC spectrum corresponding $\tau = 2$ ns slice (i.e., close to the maximum of the echo). A signal to noise ratio of 21 was obtained for this slice [42]. The ESEEM peaks can potentially interfere with the interpretation of DQC spectra for short distances.

However, ESEEM modulation may be suppressed at certain values of τ, due to the observer blind spots effect [33,34]. These values of τ, denoted by $\tau_{\alpha,\beta}$, are given by [33,34]:

$$\tau_{\alpha,\beta} = (2n+1)\pi/\omega_{\beta,\alpha}, \quad (1)$$

where, n is an integer and $\omega_{\alpha,\beta}$, the ESEEM frequencies, are:

$$\omega_{\alpha,\beta} = [(\pm A/2 - \omega_H)^2 + (B/2)^2]^{1/2}. \quad (2)$$

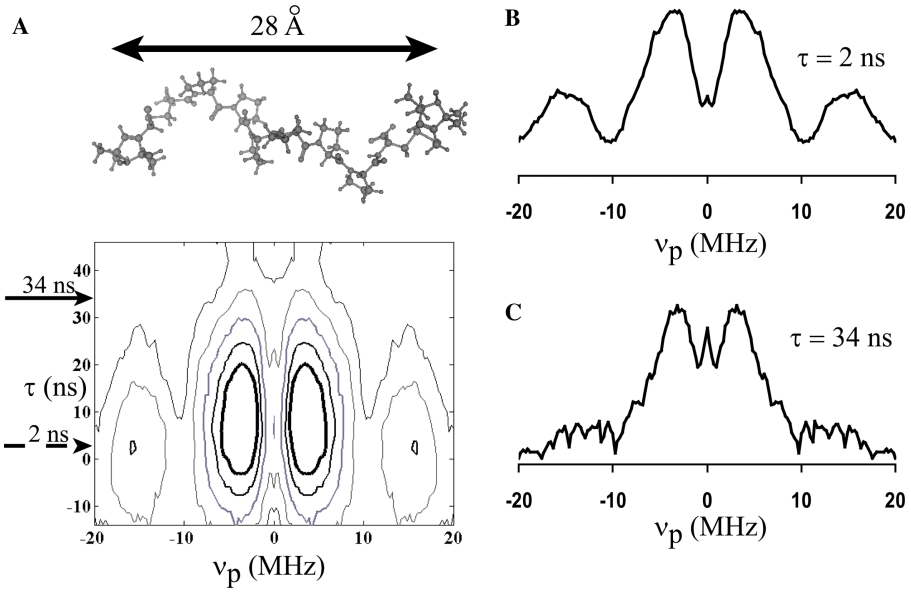

Fig. 2. (A) A contour plot of the 2D DQC spectra of CPPPPPPC peptide (shown in the inset). The ν_p dimension reports on the dipolar interaction. The orthogonal dimension, labeled τ, refers to several slices along the echo (cf. Fig. 1). The DQC spectra for slices at $\tau = 2$ and at $\tau = 34$ ns are shown in (B) and (C), respectively. The ESEEM peaks at ±14.7 MHz are suppressed for the $\tau = 34$ ns slice.

In Eq. (2), ω_H is the proton resonance frequency and A, and B are related to the A_{zz}, A_{zx}, and A_{zy} components of the electron–proton hyperfine tensor. In particular, $A = A_{zz}$ and $B = (A_{zx}^2 + A_{zy}^2)^{1/2}$ [33]. Eq. (1) is rigorously valid only for ideal non-selective pulses. However, it still provides a useful approximation provided that the lengths of the pulses, t_{pulse}, are much shorter than the nuclear modulation period, (i.e., for $t_{pulse} \ll (2\pi/\omega_H) \approx 68$ ns) [34].

For these samples, the electron spin is weakly coupled to the protons and, hence, $\omega_{\alpha,\beta} \approx \omega_H$. With $\omega_H = 9.24 \times 10^7$ (rad s^{-1}), observer blind spots can be expected for $\tau = 34$ ns ($n = 0$), $\tau = 102$ ns ($n = 1$), etc. Fig. 2C, shows the DQC spectrum corresponding to the slice at $\tau = 34$ ns. The ESEEM peaks are clearly suppressed, although the signal-to-noise ratio is reduced to about 8. This observer blind spots effect can only be exploited by transiently digitizing the echo.

In Fig. 3, DQC FTESR spectra of the organic biradical, R1, are shown for $\tau = 2$ ns and for $\tau = 34$ ns. Peaks due to electron–electron dipolar interaction occur at ±4.8–6.2 MHz, which corresponds to an average distance of ~21 Å [43]. The average intramolecular distance is consistent with the inter-nitroxide proximity of 20 ± 1 Å [40], obtained in energy minimized structural calculations using an Unrestricted Hartree–Fock approach in the CACHE software. Peaks arising from ESEEM with matrix protons occur at ±15.0 MHz, and

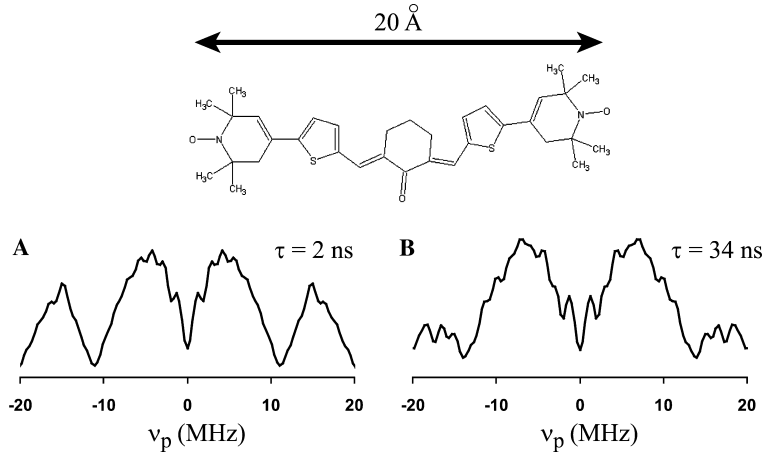

Fig. 3. DQC FTESR spectra of biradical R1 (shown in inset) for (A) $\tau = 2$ ns and (B) for $\tau = 34$ ns. The ESEEM peaks at ±15.0 MHz are largely suppressed for the case of $\tau = 34$ ns.

are clearly evident in the slice near the echo maximum (i.e., for $\tau = 2$ ns, cf. Fig. 3A). These ESEEM peaks are substantially suppressed at the observer blind spot (i.e., for $\tau = 34$ ns, cf. Fig. 3B).

4. Conclusions

We show that DQC spectra can be routinely obtained with a commercial FT-ESR spectrometer. Additionally, we demonstrate that the concept of observer blind spots readily provides DQC spectra that are free of complications from ESEEM peaks.

Acknowledgments

This work was supported by NSF CAREER Award (MCB 0346898) and the Petroleum Research Fund, administered by the American Chemical Society (37933-G4). The Howard Hughes Medical Institute is acknowledged for a Summer Undergraduate Fellowship award to JB. Soraya Pornsuwan and Andrey Tataurov are thanked for help with the data analysis.

References

[1] V.V. Khurshev, A.M. Raitsimring, Y.D. Tsvetkov, Selection of the dipolar interaction by the "2 + 1" Pulse Train ESE, J. Magn. Reson. 81 (1989) 441–454.
[2] A.D. Milov, A.G. Maryasov, Y.D. Tsvetkov, Pulsed electron double resonance (PELDOR) and its applications in free-radicals research, Appl. Magn. Reson. 15 (1998) 107–143.
[3] P.P. Borbat, J.H. Freed, Multiple-quantum ESR and distance measurements, Chem. Phys. Lett. 313 (1999) 145–154.
[4] L.J. Berliner, S.S. Eaton, G.R. Eaton (Eds.), Biological Magnetic Resonance, vol. 19, Kluwer Academic/Plenum Publisher, New York, 2000 (Chapters 8–13).
[5] J.H. Freed, New technologies in electron spin resonance, Ann. Rev. Phys. Chem. 51 (2000) 655–689.
[6] G. Jeschke, M. Pannier, A. Godt, H.W. Spiess, Dipolar spectroscopy and spin alignment in electron paramagnetic resonance, Chem. Phys. Lett. 331 (2000) 243–252.
[7] M. Pannier, S. Veit, A. Godt, G. Jeschke, H.W. Spiess, Dead-time free measurement of dipole–dipole interactions between electron spins, J. Magn. Reson. 142 (2000) 331–340.
[8] Y. Zhou, B.E. Bowler, K. Lynch, S.S. Eaton, G.R. Eaton, Interspin distances in spin-labeled metmyoglobin variants determined by saturation recovery EPR, Biophys. J. 79 (2000) 1039–1052.
[9] P.P. Borbat, A.J. Costa-Filho, K.A. Earle, J.K. Moscicki, J.H. Freed, Electron spin resonance in studies of membranes and proteins, Science 291 (2001) 266–269.
[10] L.V. Kulik, S.A. Dzuba, I.A. Grigoryev, Y.D. Tsvetkov, Electron dipole–dipole interaction in ESEEM of nitroxide biradicals, Chem. Phys. Lett. 343 (2001) 315–324.
[11] A.D. Milov, R.I. Samoilova, Y.D. Tsvetkov, V.A. Gusev, F. Formaggio, M. Crisma, C. Toniolo, J. Raap, Spatial distribution of spin-labeled Trichogin GA IV in the gram-positive bacterial cell membrane determined from PELDOR data, Appl. Magn. Reson. 23 (2002) 81–95.
[12] G.L. Millhauser, Selective placement of electron spin resonance spin labels: new structural methods for peptides and proteins, Trends Biochem. Sci. 17 (1992) 448–452.
[13] W.L. Hubbell, C. Altenbach, Site-directed spin labeling of membrane proteins, in: S.H. White (Ed.), Membrane Protein Structure: Experimental Approaches, Oxford, New York, 1994.
[14] L. Columbus, W.L. Hubbell, A new spin on protein dynamics, Trends Biochem. Sci. 27 (2002) 288–295.
[15] W.L. Hubbell, C. Altenbach, C.M. Hubbell, H.G. Khorana, Rhodopsin structure, dynamics, and activation: a perspective from crystallography, site-directed spin labeling, sulfhydryl reactivity, and disulfide cross-linking, Adv. Protein Chem. 63 (2003) 243–290.
[16] M. Persson, J.R. Harbridge, P. Hammarstrom, R. Mitri, L.G. Martensson, U. Carlsson, G.R. Eaton, S.S. Eaton, Comparison of electron paramagnetic resonance methods to determine distances between spin labels on human carbonic anhydrase II, Biophys. J. 80 (2001) 2886–2897.
[17] P.P. Borbat, H.S. Mchaourab, J.H. Freed, Protein structure determination using long-distance constraints from double-quantum coherence ESR: study of T4 lysozyme, J. Am. Chem. Soc. 124 (2002) 5304–5314.
[18] G. Jeschke, C. Wegener, M. Nietschke, H. Jung, H.-J. Steinhoff, Interresidual distance determination by four-pulse double electron–electron resonance in an integral membrane protein: the Na^+/proline transporter PutP of *Escherichia coli*, Biophys. J. 86 (2004) 2551–2557.
[19] O. Schiemann, A. Weber, T. Edwards, T. Prisner, S. Sigurdsson, Nanometer distance measurements on RNA using PELDOR, J. Am. Chem. Soc. 125 (2003) 3434–3435.
[20] O. Schiemann, N. Piton, Y. Mu, G. Stock, J.W. Engels, T.F. Prisner, A PELDOR-based nanometer distance ruler for oligonucleotides, J. Am. Chem. Soc. 126 (2004) 5722–5729.
[21] E. Narr, A. Godt, G. Jeschke, Selective measurements of a nitroxide–nitroxide separation of 5 nm and a nitroxide-copper separation of 2.5 nm in a terpyridine based copper(II) complex by pulse EPR spectroscopy, Angew. Chem. Intl. Ed. 41 (2002) 3907–3910.
[22] G. Jeschke, Distance measurements in the nanometer range by pulse EPR, Chem. Phys. Chem. 3 (2002) 927–932.
[23] G. Jeschke, Determination of the nanostructure of polymer materials by electron paramagnetic resonance spectroscopy, Macromol. Rapid Commun. 23 (2002) 227–246.
[24] I.M.C. vanAmsterdam, M. Ubbink, G.W. Canters, M. Huber, Measurement of a Cu–Cu distance of 26 angstroms by a pulsed EPR method, Angew. Chem. Intl. Ed. 42 (2003) 62–64.
[25] M. Bennati, A. Weber, J. Antonic, D.L. Perlstein, J. Robblee, J. Stubbe, Pulsed ELDOR spectroscopy measures the distance between the two tyrosyl radicals in the R2 subunit of the *E. coli* ribonucleotide reductase, J. Am. Chem. Soc. 125 (2003) 14988–14989.
[26] A.D. Milov, A.G. Maryasov, Y.D. Tsvetkov, J. Raap, Pulsed ELDOR in spin-labeled polypeptides, Chem. Phys. Lett. 303 (1999) 135–143.
[27] A.D. Milov, Y.D. Tsvetkov, F. Formaggio, M. Crisma, C. Toniolo, J. Raap, Self-assembling properties of membrane-modifying peptides studied by PELDOR and CW-ESR spectroscopies, J. Am. Chem. Soc. 122 (2000) 3843–3848.
[28] A.D. Milov, Y.D. Tsvetkov, F. Formaggio, M. Crisma, C. Toniolo, J. Raap, The secondary structure of a membrane-modifying peptide in a supramolecular assembly studied by PELDOR and CW-ESR spectroscopies, J. Am. Chem. Soc. 123 (2001) 3784–3789.
[29] P.P. Borbat, J.H. Freed, Double-Quantum ESR and Distance Measurements, in: L.J. Berliner, S.S. Eaton, G.R. Eaton (Eds.), Biological Magnetic Resonance, vol. 19, Kluwer Academics/Plenum Publishers, New York, 2000, pp. 383–459.

[30] M. Fedin, M. Kalin, I. Gromov, A. Schweiger, Applications of π-photon-induced transparency in two-frequency pulse electron paramagnetic resonance experiments, J. Chem. Phys. 120 (2004) 1361–1368.
[31] C. Elsasser, M. Brecht, R. Bittl, Pulsed electron–electron double resonance on multinuclear metal clusters: assignment of spin projection factors based on the dipolar interaction, J. Am. Chem. Soc. 124 (2002) 12606–12611.
[32] P.P. Borbat, R.H. Crepeau, J.H. Freed, Multifrequency two-dimensional fourier transform ESR: An X/Ku-Band spectrometer, J. Magn. Reson. 127 (1997) 155–167.
[33] C. Gemperle, A. Schweiger, R.R. Ernst, Novel analytical treatments of electron spin-echo envelope modulation with short and extended pulses, J. Magn. Reson. 91 (1991) 273–288.
[34] A. Schweiger, G. Jeschke, Principles of Pulse Electron Paramagnetic Resonance, Oxford University Press, 2001 p. 260.
[35] A.P. Todd, G.L. Millhauser, ESR spectra reflect local and global mobility in a short spin-labeled peptide throughout the alpha helix-coil transition, Biochemistry 30 (1991) 5515–5523.
[36] J.R. Klauder, P.W. Anderson, Spectral diffusion decay in spin resonance experiments, Phys. Rev. 125 (1962) 912–932.
[37] R.G. Larsen, D.J. Singel, Double electron–electron resonance spin-echo modulation spectroscopic measurement of electron-spin pair separations in orientationally disordered solids, J. Chem. Phys. 98 (1993) 5134–5146.
[38] We found subtraction of an exponential decay sufficient to remove contributions from transverse relaxation and decay due to intermolecular electron–electron interactions.
[39] S.A. Dikanov, Y.D. Tsvetkov, Electron Spin Echo Envelope Modulation (ESEEM) Spectroscopy, CRC Press, Boca Raton, FL, 1992.
[40] The energy was minimized from various starting geometries and the uncertainties reflect the range of distances obtained in the different energy minimized conformations.
[41] L.V. Kulik, I.A. Grigoryev, E.S. Salnikov, S.A. Dzuba, Y.D. Tsvetkov, Electron spin-echo envelope modulation induced by slow intramolecular motion, J. Phys. Chem. A 107 (2003) 3692–3695.
[42] To determine the noise we chose the spectral range between 21 and 26 MHz (cf. Fig. 2B), which contains some spectral components. These were eliminated by subtracting a second order polynomial from the spectrum. The noise was determined from the resultant baseline.
[43] Despite the 2.5 mM concentration of this sample, we do not expect nor observe low frequency peaks due to intermolecular dipolar interactions. The average intermolecular distance between paramagnetic centers is ~90 Å assuming a homogeneous distribution of molecules.